Molecular Cancer Therapeutics

# A Bifunctional MAPK/PI3K Antagonist for Inhibition of Tumor Growth and Metastasis

Stefanie Galbán[1,2], April A. Apfelbaum[1,2], Carlos Espinoza[1,2], Kevin Heist[1,2], Henry Haley[1,2], Karan Bedi[3], Mats Ljungman[3], Craig J. Galbán[1,2,4], Gary D. Luker[1,2,5], Marcian Van Dort[1,2], and Brian D. Ross[1,2,6]

## Abstract

Responses to targeted therapies frequently are brief, with patients relapsing with drug-resistant tumors. For oncogenic MEK and BRAF inhibition, drug resistance commonly occurs through activation of PI3K/AKT/mTOR signaling and immune checkpoint modulation, providing a robust molecular target for concomitant therapy. Here, we evaluated the efficacy of a bifunctional kinase inhibitor (ST-162) that concurrently targets MAPK and PI3K signaling pathways. Treatment with ST-162 produced regression of mutant KRAS- or BRAF-addicted xenograft models of colorectal cancer and melanoma and stasis of BRAF/PTEN–mutant melanomas. Combining ST-162 with immune checkpoint blockers further increased efficacy in a syngeneic KRAS-mutant colorectal cancer model. Nascent transcriptome analysis revealed a unique gene set regulated by ST-162 related to melanoma metastasis. Subsequent mouse studies revealed ST-162 was a potent inhibitor of melanoma metastasis to the liver. These findings highlight the significant potential of a single molecule with multikinase activity to achieve tumor control, overcome resistance, and prevent metastases through modulation of interconnected cell signaling pathways. *Mol Cancer Ther; 16(11); 2340–50. ©2017 AACR.*



## Introduction

To maximize responses to emerging therapies, such as molecularly targeted small molecules and immunotherapy, initial tumor profiling to identify patients most likely to respond is a key recommendation of the NCI "Cancer Moonshot" (1). Well-known oncogenic processes, including aberrant hyperactivation of the MAPK pathway by KRAS or BRAF mutations, initiate tumor growth and progression in colorectal cancer, melanoma, and many other human tumors (2). Although MEK and BRAF inhibitors have produced brief remissions in melanoma, rather modest responses have been observed in colorectal cancers when used as a single targeted therapy. Emerging resistance may limit durable tumor control as tumor relapse may occur due to intrapathway regulatory loops and signaling pathway cross-talk, which may limit clinical success of targeted inhibitors (3). For example, PI3K represents a major signaling node activated by MEK inhibitors (MEKi), and inhibition of PI3K has been shown to forestall the onset of MEKi resistance (4–9). Furthermore, activation of AKT by relief of negative feedback mechanisms (MEKi) or loss of PTEN promotes metastasis. Therefore, the PI3K signaling pathway represents an important target in management of metastasis-related mortalities, thus warranting cotargeting of MAPK and PI3K pathways. The PI3K/AKT pathway is highly active in melanoma, and elevated phosphorylation levels of AKT (pAKT) are associated with a higher risk of metastatic disease (10, 11). These data underscore the need to cotarget both MAPK and PI3K pathways to further improve therapeutic outcomes.

Rapid progress in genomics and genetic profiling of patient tumor tissue has yielded a deluge of new targets for drug discovery and development. Several promising kinase inhibitors have been developed and advanced to clinical trials and practice over the past decades (12). As an approach toward multikinase targeting, a prototype bifunctional inhibitor (ST-162; previously designated as compound 14) was designed on the basis of computational docking studies using structural analogues of a potent PI3K inhibitor ZSTK474 and an MEK inhibitor PD0316684 (an analogue of PD0325901) as templates with subsequent covalent linking of the active pharmacophores (13). Thus, ST-162 exhibits bifunctional allosteric noncompetitive MEK inhibition with simultaneous ATP-competitive PI3K inhibition (13).

Here, we explored the anticancer therapeutic activity of ST-162 and its impact on simultaneous targeting of MEK and PI3K signaling. *In vivo* efficacy studies in colorectal and melanoma mouse xenograft models demonstrated significant growth inhibition could be achieved. Further studies evaluating the combination of ST-162 with immune checkpoint blockers demonstrated significant tumor growth inhibition in a syngeneic colorectal xenograft model. Broad transcriptome studies suggest ST-162 regulates genes involved in metastases, indicating potential for this compound to control metastatic disease. In fact, treatment of a metastatic mouse model with ST-162 was shown to markedly

[1]Center for Molecular Imaging, The University of Michigan Medical School, Ann Arbor, Michigan. [2]Department of Radiology, The University of Michigan Medical School, Ann Arbor, Michigan. [3]Department of Radiation Oncology, The University of Michigan Medical School, Ann Arbor, Michigan. [4]Department of Biomedical Engineering, The University of Michigan Medical School, Ann Arbor, Michigan. [5]Department of Microbiology and Immunology, The University of Michigan Medical School, Ann Arbor, Michigan. [6]Department of Biological Chemistry, The University of Michigan Medical School, Ann Arbor, Michigan.

**Note:** Supplementary data for this article are available at Molecular Cancer Therapeutics Online (http://mct.aacrjournals.org/).

**Corresponding Author:** Brian D. Ross, The University of Michigan Medical School, University of Michigan, Ann Arbor, MI 48109. Phone: 734-763-2099; Fax: 734-763-5447; E-mail: bdross@med.umich.edu

**doi:** 10.1158/1535-7163.MCT-17-0207

reduce melanoma hepatic metastasis, highlighting a potential therapeutic strategy to block this fatal end-stage disease process. The bifunctional inhibitor significantly attenuated tumor cell growth and metastasis, identifying a new class of small molecules as a novel direction for simultaneous targeting of key oncogenic pathways such as MEK and PI3K.

## Materials and Methods

### Materials

PD0325901 (901) and ZSTK474 (ZSTK) were purchased from Cayman Chemicals. Experimental compound ST-162 was custom synthesized by Cayman Chemicals. Stock solutions (10 mmol/L) of ST-162, ZSTK474 (representative PI3K inhibitor), and PD0325901 (representative MEK inhibitor) were prepared in DMSO and used to make final solutions by serial dilution in media. Control wells were incubated with media containing 0.1% DMSO carrier solvent.

### Cell lines

Human A2058, A375 melanoma cells, and murine CT26 were obtained from the ATCC (2016, CRL-11147, CRL-1619, CRL-2638) and grown in supplemented (10% FBS, 1% penicillin-streptomycin) DMEM or RPMI1640 (Gibco, Thermo Fisher Scientific) media, respectively, and maintained at 37°C in an atmosphere of 5% $CO_2$. A2058 melanoma cells were infected with lentivirus pLVX-EF1aLuc2-IRES-blast described previously (14) and selected for blastacidin resistance by supplementing the media with 10 μg/mL blastacidin (Gibco).

### Immunoblot analysis

Cells were seeded in 6-well or 10-cm dishes 24 hours prior to treatment and incubated with the respective inhibitor solutions for 1 hour or as otherwise indicated. Cells were washed with PBS and lysed with RIPA lysis buffer supplemented with protease inhibitors (Complete Protease Inhibitor Cocktail, Roche) and phosphatase inhibitors (PhosSTOP, Roche). Tumor tissue was homogenized directly in RIPA buffer and sonicated. Protein concentrations of whole-cell lysates were determined using Lowry assays (Bio-Rad). Lysates of equal protein concentrations were prepared in LDS sample buffer (Invitrogen), separated on denaturing Bis-Tris gel (Invitrogen), and transferred to nitrocellulose membranes (GE Healthcare). Membranes were blocked in 5% milk in 0.1% Tween 20 Tris-buffered saline (TBST) and subsequently incubated with primary antibodies against phospho-p44/42 MAPK (pErk1/2; Thr202/Tyr204), pAKT S473, total ERK, or total AKT (Cell Signaling Technology) in TBST overnight at 4°C. Following washing with TBST, membranes were incubated with appropriate secondary HRP-conjugated antibodies form Jackson ImmunoResearch in 2.5% milk in TBST for 1 hour at room temperature. Once washed, membranes were analyzed using ECL or ECL-Plus substrate from Pierce to detect the activity of peroxidase according to the manufacturer's instructions (Amersham Pharmacia).

### *In vitro* MEK1 kinase assay

*In vitro* MEK1 kinase inhibition by inhibitor analogues was determined using a standard kinase assay reaction and Kinase-Glo Luminescent Kinase Assay Kit from Promega. Kinase reactions were carried out with purified recombinant active MEK1-GST (cat #: M8822, Sigma-Aldrich) and inactive Erk2 (cat #: PV3314, Thermo Fisher Scientific) in kinase reaction buffer (ab189135, Abcam) supplemented with 0.25 mmol/L DTT. In brief, inhibitors were preincubated with recombinant MEK1 at a final concentration of 4 μg/mL at room temperature for 30 minutes prior to addition of inactive substrate (Erk2) and ATP at final concentration of 0.025 μg/μL and 10 μmol/L, respectively. Reactions were incubated at room temperature for 2 hours before equal volumes of Kinase-Glo solution were added to each well and incubated for 30 minutes in the dark. Bioluminescence was measured on an Envision multilabel reader from PerkinElmer. Assays were conducted in triplicate with various inhibitor concentrations each run in duplicate. $IC_{50}$ data were calculated using GraphPad Prism software (version 7.0a). Data represent three independent experiments with SEM.

### *In vitro* PI3K kinase assay

Quantitation of PI3Kα lipid kinase activity was carried out by Life Technologies with purified enzyme using the fluorescence-based Adapta TR-FRET assay (assay-# 1014) protocol. Assays were conducted in triplicate with various inhibitor concentrations (0.1 nmol/L–10 μmol/L).

### Growth-inhibitory $IC_{50}$

A total of 5,000 cells per well in 100 μL were plated in 96-well plates and treated with inhibitors 24 hours postseeding. Cells were treated for 72 hours with inhibitors at various concentrations (0–10 μmol/L 901, 0–50 μmol/L for ZSTK, and ST-162) in triplicate. Cell viability was assessed using CellTiter-Glo Reagent (Promega), and bioluminescence was measured using an Envision multi-label plate reader (PerkinElmer). Viability was calculated as a percentage of the DMSO-treated cells. Assays were conducted at least three times with various inhibitor concentrations each run in triplicate. Growth-inhibitory (GI) $IC_{50}$s were calculated using GraphPad Prism software (Version 5.0). The GI-$IC_{50}$ value was determined by fitting a log (inhibitor) versus response (variable slope) curve to the data using GraphPad Prism 7. Error bars represent SEM from three independent experiments.

### BrUrd-seq for transcriptome analysis

A2058 melanoma cells were incubated with 10 μmol/L PD325901, ZSTK474, combination of 901 + ZSTK, 20 μmol/L ST-162, or equimolar DMSO for 2 hours. The bromouridine sequencing (BrUrd-seq) procedure has been described previously (15, 16). In brief, nascent RNA was labeled by adding 2 mmol/L BrUrd to the media for the last 30 minutes of the drug treatment; then, cells were lysed in TRIzol reagent (Invitrogen) and total RNA was isolated. BrUrd-labeled, nascent RNA was isolated using anti-BrUrd antibodies (BD Biosciences) conjugated to magnetic beads (Invitrogen). The BrUrd-labeled RNA was then used to generate strand-specific cDNA libraries that were sequenced at the University of Michigan Sequencing Core using an Illumina (San Diego, CA) HiSeq 2000 sequencer as described previously (15, 16). GSEA was used to identify up- and downregulated gene sets by determining which associated genes were significantly enriched in each gene set. The log fold change in expression of genes $\geq$300 bp and expressed $\geq$0.5 RPKM was used as the ranking metric by GSEA. The gene sets were obtained from version 4.0 of the Molecular Signatures Database (http://www.broadinstitute.org/gsea/msigdb/index.jsp). Gene sets with FDR corrected $P$ values <0.01 were considered to be significantly enriched and were used in the analysis.

### Mouse models

Female nude-Foxn1nu (Envigo), 4 to 6 weeks old were used for A2058 and A375 melanoma and CT26 colorectal xenograft models. Mice were housed under pathogen-free conditions and all procedures involving animals and their care were approved by the University Committee on the "Use and Care of Animals" (UCUCA) at the University of Michigan (An Arbor, MI). Flank xenograft models were generated by subcutaneous injection of 2–5 $\times$ $10^6$ viable A2058, A375 melanoma, or murine colon carcinoma CT26 cells together with reconstituted basement membrane BD Matrigel Basement Membrane Matrix (Becton, Dickinson and Company). Each experimental group included a minimum of 4 to 6 tumors (2 flank tumors per animal). Treatment was started when tumor mass reached 50 to 150 $mm^3$. Vehicle-treated animals were treated with 200 μL ORA-Plus (Perrigo) suspension by oral gavage. PD0325901 and ZSTK474 were purchased from Cayman Chemicals and administered as suspension orally at a dose of 5 and 100 mg/kg, respectively. Experimental ST-162 was given at a dose of 400 mg/kg orally daily. All drugs were resuspended in 200 μL ORA-Plus and given daily for 14 days unless otherwise indicated in the figure legends. Tumor tissue was excised and formalin fixed for histology or snap frozen and processed in RIPA buffer for Western blotting. Tumor growth was measured by MRI (see below). Treatment tolerability was defined as loss of body weight less than 10% of initial weight. Kaplan–Meier plots were generated in GraphPad.

Four- to 6-week-old female BALB/C mice (Charles River Laboratories) were used to establish the CT26 murine colorectal carcinoma syngeneic mouse model. Tumors were established by subcutaneously implanting 1–5 $\times$ $10^6$ CT26 cells in 1:1 suspension with Matrigel into the right and left flank of mice. Treatments as indicated in figure legends began at day 7 postimplantation or when tumor size reached 50 to 150 $mm^3$. PD-1 (RMP1-14) and rat IgG2a (2A3) isotype control antibodies were purchased from BioCell. Antibodies were administered twice per week (Monday and Thursday) by intraperitoneal injections, whereas ST-162 and ORA-Plus were administered by oral gavage daily. Tumor volumes were measured by MRI as described below. Mice were euthanized when tumor ulceration occurred or animals reached predetermined experimental endpoints. Treatment tolerability was defined as loss of body weight less than 10% of initial weight.

For assessment of ST-162 against metastatic disease, A2058-luciferase–expressing cells (1 $\times$ $10^5$) were introduced to male NSG mice by intracardiac injection in 100 μL serum free media as described previously (17). Tumor growth was assessed using bioluminescence imaging beginning at 24 hours postimplantation.

### MRI evaluation of tumor treatment responses

MRI was performed using a 9.4-T, 16-cm horizontal bore (Agilent Technologies, Inc.) Direct Drive System with a mouse head quadrature volume coil or mouse surface receive coil (m2m Imaging, Corp) actively decoupled to a whole-body volume transmit coil (Rapid MR International, LLC). Throughout the MRI experiments, animals were anesthetized with 1% to 2% isoflurane/air mixture, and body temperature was maintained using a heated air system (Air-Therm Heater; World Precision Instruments). MR images were acquired before treatment initiation, then twice a week until the animals were sacrificed or became moribund. MRI was used to quantify tumor volumes over time. For longitudinal quantification of tumor volumes, volumes of interest were contoured along the enhancing tumor rim using the contrast-enhanced T1-weighted images. Absolute tumor volumes were plotted for each treatment group as function of time.

### Bioluminescence imaging

Mice were imaged at 0, 3, 6, and 10 days after intracardiac implantation of A2058-luciferase–expressing cells. Imaging was performed on an IVIS Spectrum from PerkinElmer. Mice were injected with D-luciferin (150 mg/kg, Promega) solution in PBS and anesthetized with 1% to 2% isoflurane/air while imaged. Images were acquired at 10 minutes after injection to capture peak luminescence. Regions of interest were drawn around the entire mouse, and a highest photon emission value for each image was used for analysis.

### Statistical analysis

Group comparisons in proliferation plots were performed using a two-way ANOVA controlling for multiple comparisons using a Bonferoni *post hoc* test. Results were declared statistically significant at the two-tailed 5% comparison-wise significance level ($P < 0.05$). All data are presented as mean values $\pm$ SEM. Statistical analysis was performed using PRISM 6 (GraphPad Software, Inc.).

## Results

### Bifunctional kinase inhibition demonstrates efficacy in a KrasG12D colorectal xenograft model

*KRAS* mutations in cancer result in activation of the MAPK/ERK kinase pathway, conferring sensitivity to MEKi (18). Initial studies were performed to examine the efficacy of ST-162 in a KrasG12D-driven colon cancer (CT26) cell line. Western blotting and densitometry of cell lysates from cells treated with the MEK inhibitor PD0325901 (901), the pan-PI3K inhibitor ZSTK474 (ZSTK), combination of both (901 + ZSTK) or ST-162 indicate that ST-162 simultaneously inhibited phosphorylation of ERK (pERK1/2) and AKT (pAKT(S473); (Fig. 1A and B) when compared with single agents and analogous to combination treatment (901 + ZSTK). Furthermore, Western blotting and corresponding densitometry performed on excised tumor tissue from a CT26 xenograft at 2 hours following a single oral dose of ST-162 (400 mg/kg) revealed *in vivo* targeting of ERK phosphorylation by the MEKi pharmacophore of the bifunctional inhibitor (Fig. 1C and D) was achieved. Levels of pAKT were below the detection limits, indicating that AKT plays a rather negligible role in CT26 colorectal oncogenesis when compared with MEK. This statement is supported by the next experiment wherein we evaluated efficacy of ST-162 for tumor growth reduction in the CT26 xenograft model. The treatment schedule as depicted in Fig. 1E was used to compare ST-162 with single-agent therapies (901) or (ZSTK) and combination therapy (901 + ZSTK). Tumor volumes quantified by MRI revealed that ZSTK474 alone had no significant effect on tumor growth in this KRAS-addicted xenograft model when compared with vehicle control–treated animals (Fig. 1F). However, significant tumor growth inhibition ($P < 0.0001$) was observed when treated with 901 alone. Combination therapy (901 + ZSTK) and ST-162 both produced reductions in tumor growth that were indistinguishable from 901 over the 16-day treatment period. These data show that chemical linkage to ZSTK

did not limit *in vivo* efficacy of the 901 pharmacophore in ST-162, which was shown in Fig. 1F to be active in this tumor model.

Mounting evidence suggests that KrasG12D-addicted tumors can be targeted by MEK inhibitors, but over time, emergence of resistance may occur through activation of alternate pathways, such as PI3K. Although we did not observe PI3K activation of resistance on the timescale of this short-term initial experiment, this study illustrates that ST-162 produced equivalent antitumor effects as compound 901 *in vivo* in this tumor model.

### Combination of ST-162 with immune checkpoint blockade provides enhanced efficacy in a syngeneic colon tumor model

Upregulation of immune checkpoint signaling molecules, such as PD-L1, is a significant contributing factor to treatment

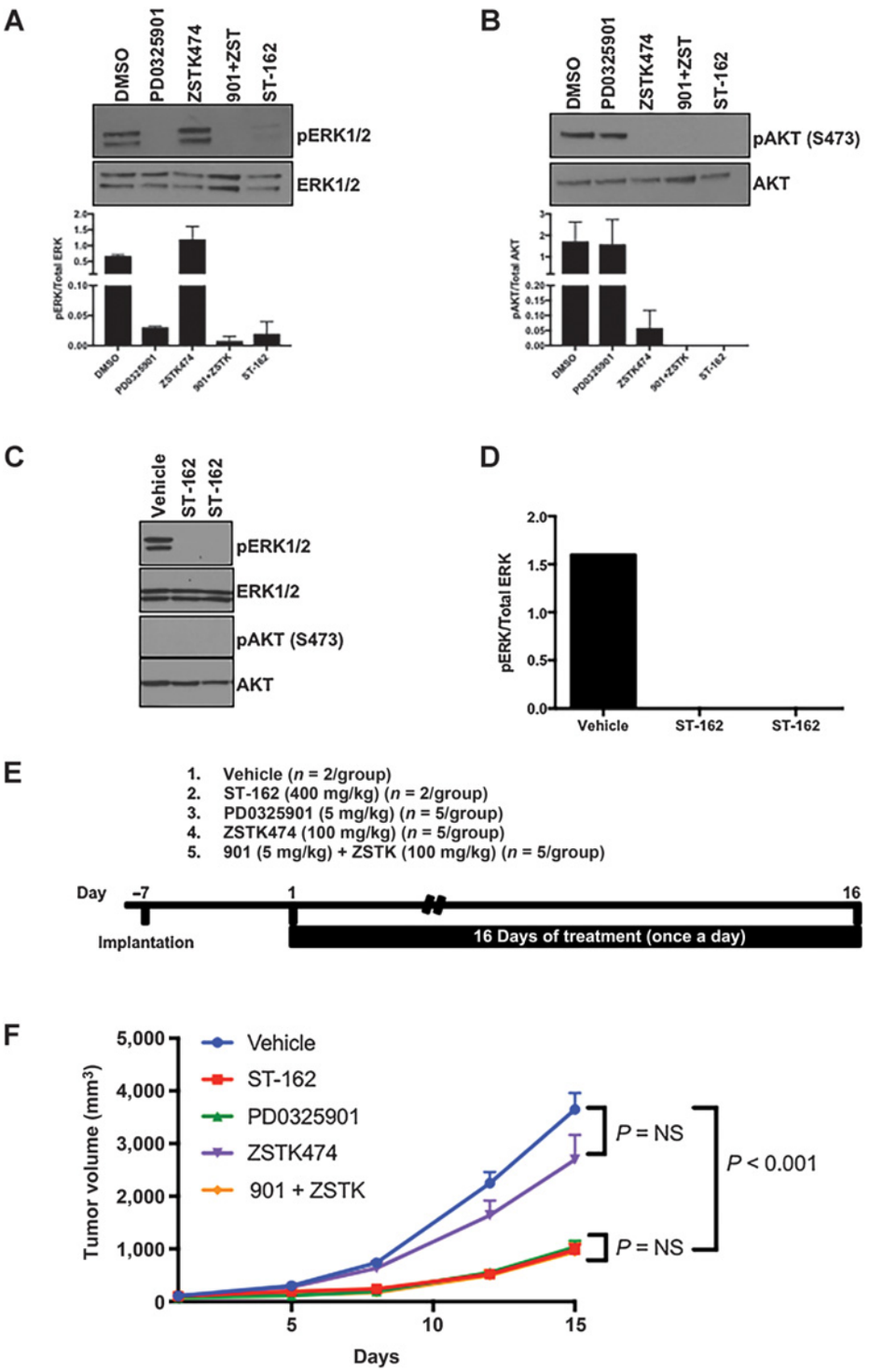


**Figure 1.**
Antitumor activity of bifunctional inhibitor in murine colorectal xenograft model. **A** and **B,** Western blotting and densitometry of cell lysates from CT26 cells treated with 10 μmol/L 901, ZSTK, combination of both (901 + ZSTK, 10 μmol/L each), or 20 μmol/L of ST-162. Presented data are compiled from two independent Western blots with mean values ± SEM. **C,** Western blotting of tumors from CT26 xenografts. Approximately 100 $mm^3$ tumor–bearing animals were treated with 400 mg/kg ST-162 or vehicle for 2 hours prior to tumor excision and processing for analysis. **D,** Densitometry of Western blot presented in **C**. Presented data are from one Western blot of tumor samples from two ST-162–treated mice and one untreated mouse. **E,** Experimental design ($n = 2$ for vehicle and ST-162–treated groups and $n = 5$ for all other groups; each mouse was injected with CT26 cells into the right and left flank/2 tumors per animal). Treatment was initiated 7 days after CT26 implantation, indicated as day 1 of drug treatment. Mice were treated orally once daily for 16 days with vehicle, 400 mg/kg ST-162, 5 mg/kg 901, 100 mg/kg ZSTK474, or combination of 901 + ZSTK (5 and 100 mg/kg, respectively). **F,** Tumor growth inhibition during 16 days of treatment as measured by MRI. ZSTK474 alone had no significant effect on tumor growth when compared with vehicle control–treated animals (ns). Significant tumor growth inhibition ($P < 0.0001$) was observed between control and 901-treated animals. Combination therapy (901 + ZSTK) and ST-162 both produced reductions in tumor growth that were indistinguishable from 901 over the 16-day treatment period (ns).

failures in a variety of neoplasms (19, 20). Here, we explored whether blocking immune checkpoint regulation synergizes with targeted MAPK/PI3K therapy. For this purpose, we established a murine colorectal CT26 mouse model previously published by Liu and colleagues (21) and utilized to assess BRAF and MEK inhibition in combination with immunomodulatory antibodies like anti–PD-1 (21).

First, we investigated *in vivo* effects of MAPK/PI3K inhibition in combination with immunomodulatory antibodies in the murine immunocompetent BALB/c syngeneic CT26 tumor model. Figure 2A shows treatment schedule and doses, with Fig. 2B showing changes in tumor volumes as quantified by MRI over the time course of treatment. Twenty-one days of treatment with anti–PD-1 antibody alone resulted in moderate antitumor activity, while treatment with ST-162 alone limited tumor growth to a greater extent. Significant inhibition of tumor growth occurred in animals treated with combined ST-162 and anti–PD-1 antibody when compared with vehicle control ($P < 0.0001$) or anti–PD-1 alone ($P = 0.02$; Fig. 2C), whereas no statistical significance could be determined when compared with ST-162 alone. No toxicity, defined as more than 10% of body weight loss, was noted in any of the treatment groups (21). A Kaplan–Meier plot depicting tumor progression (progression noted when tumor volumes increased to 600% of initial pretreatment volume) revealed a statistically significant advantage ($P < 0.05$) by combining ST-162 with anti–PD-1 immune therapy (Fig. 2C).

### Assessment of *in vitro* and *in vivo* PI3K and MEK inhibition

*In vitro* MEK1 and PI3Kα enzyme assays with ST-162 (22, 23) were performed to assess inhibition of PI3Kα and MEK1 by using competitive and noncompetitive kinase assays, respectively. $IC_{50}$s were determined as 191 nmol/L (±64 nmol/L) for PI3Kα and 398 nmol/L (±1.42 nmol/L) for MEK1. Inhibition were the average of three experiments each conducted in duplicate. Data reported as mean ± SEM. Next, we undertook studies to compare the efficacy of ST-162 in melanoma cells with BRAF V600E and PTEN wild-type (PTENwt; A375) mutations or melanoma cells with known PTEN-null ($PTEN^-$) status (A2058). Comparison of growth inhibition in PTENwt versus $PTEN^-$ melanoma cells (Table 1) as measured using the CellTiter-Glo viability assay showed similar GI-$IC_{50}$ values for both cell lines.

### Dual kinase inhibition produces tumor growth reduction in PTEN-null tumors and regression in PTEN wild-type melanoma xenografts

Here, we evaluated the efficacy of ST-162 in melanoma cells in inhibiting AKT and ERK phosphorylation as surrogates of PI3K and MEK inhibition by Western blotting. Melanoma (A375 and A2058) cell treatment with ST-162 resulted in simultaneous inhibition of AKT and ERK phosphorylation similar to inhibition observed by combination treatment of 901 and ZSTK (Fig. 3A and B). However, when cells were treated with 901 or ZSTK alone, pathway-specific inhibition (ERK and AKT, respectively) was observed, but as expected no inhibition of the other pathway. This indicates efficiency of ST-162 in attenuating the enzymatic activity of PI3K and MEK.

We next evaluated effects of ST-162 on melanoma xenografts with activation of both MAPK and PI3K/AKT signaling through mutations in BRAF and PTEN. The schematic depicts the treatment schedule for mice with A375 and A2058 melanoma cells implanted into the right and left flanks, respectively, of immunocompromised mice (Fig. 3C). ST-162 treatment of the A375 xenograft model with MAPK signal activation caused tumor regression over the 14-day treatment period, as evidenced by a loss of tumor volume from the pretreatment value (Fig. 3D). ST-162 also significantly reduced progression of A2058 tumors relative to vehicle control (Fig. 3E). These data show efficacy of ST-162 against melanomas with constitutive activation of MAPK signaling or both MAPK and PI3K pathways.

### Comprehensive nascent transcriptome analysis of melanoma cells treated with ST-162

To identify potential signaling events induced by MAPK/PI3K inhibition with ST-162 relative to combination treatment (901 + ZSTK) or single agents alone, we employed a comprehensive transcriptome analysis utilizing a nascent RNA sequencing approach (BrUrd-seq). In brief, nascent RNA was labeled with BrUrd, pulled down with anti-BrUrd antibody conjugated to magnetic beads, converted into a cDNA library, and sequenced as described previously (15, 16). For our studies, A2058 cells were treated with single agents (901, ZSTK), combination (901 + ZSTK), or ST-162 for 2 hours where BrUrd was added to the cells 1.5 hours into the treatment. After 30 minutes of BrUrd labeling, we collected cells and isolated nascent RNA (Fig. 4A). A heatmap of 1,481 genes modulated more than 2-fold in treated cells compared with vehicle control (DMSO) was generated from the Bru-Seq data showing clustering of ST-162–treated cells with cells treated with ZSTK or combination therapy (Fig. 4B). These findings reveal gene activation/inhibition of signaling events similarly modulated by ST-162, ZSTK, and combination therapy (901 + ZSTK) as compared with 901. Results from gene set enrichment analysis (GSEA) derived from the KEGG pathway database performed with the BrUrd-Seq data obtained from A2058 melanoma cells treated with 901 alone indicates upregulation of the mTOR- and phosphatidylinositol signaling pathways (Supplementary Fig. S1A), which previously have been identified as mechanisms of drug resistance in cancer cells treated with MEK inhibitors (3, 24–28). These data reinforce the need for combined inhibition of both MEK and PI3K/mTOR pathways in cancer therapy. No change in transcription of genes in the PI3K/AKT/mTOR pathway was observed in cells treated with ST-162 or in cells treated with the combination of single agents (Supplementary Fig. S1C and S1D). Interestingly, genes in the pathways such as p53 signaling and cell-cycle regulation were found transcriptionally upregulated in all PI3K-inhibited cells (ZSTK, 901 + ZTK, ST-162), but not in MEK-inhibited cells (901; Supplementary Fig. S1B–S1E).

GSEA–KEGG pathway analyses depicted pathways transcriptionally downregulated by all treatments (Supplementary Fig. S1F–S1J). Cells treated with 901 showed pathway downregulation of ECM receptor interaction, focal adhesion, TGFβ signaling, base excision repair, and apoptosis (Supplementary Fig. S1F, S1H, and S1I), whereas mTOR signaling was downregulated in all cells treated with ZSTK (Supplementary Fig. S1J). In summary, this comprehensive transcriptome analysis revealed differences between molecularly targeted monotherapies and combined MEK and PI3K inhibition. Interestingly, transcriptional differences in genes and pathways regulation were identified between inhibiting MAPK and PI3K using combined agents

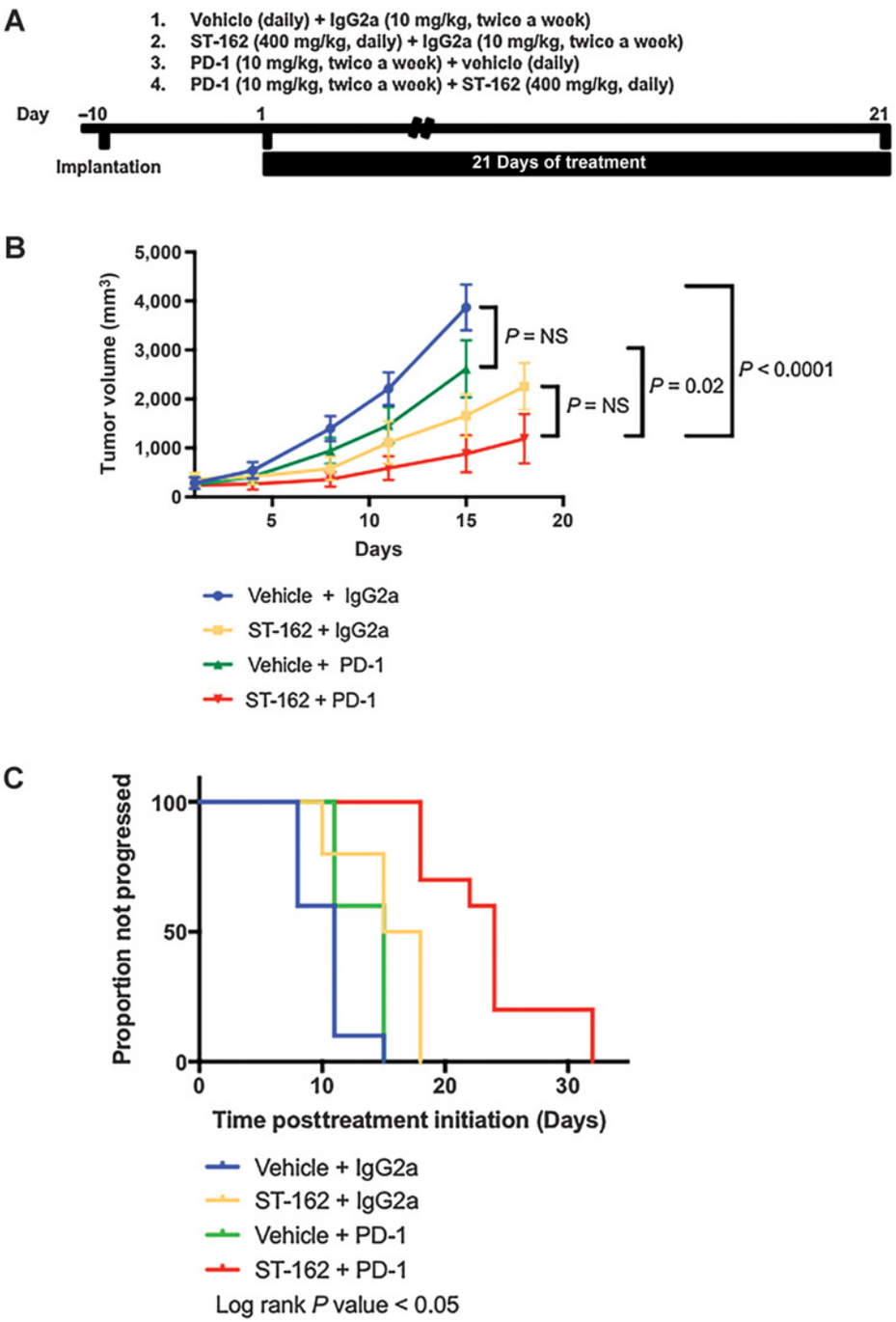


**Figure 2.**
Tumor growth regression by combination of immunomodulators PD-1 and bifunctional MAPK/PI3K inhibitor in murine syngeneic model. **A,** Experimental design ($n = 5$/treatment group/2 tumors per animal). Treatment was initiated 10 days after CT26 implantation, indicated as day 1 of drug treatment. Mice were treated orally once daily for 21 days with vehicle, 400 mg/kg ST-162, or twice a week with antibodies against PD-1 or control IgG2 as indicated in the schematic. **B,** Tumor growth inhibition during 21 days of treatment measured by MRI. Significant inhibition of tumor growth occurred in animals treated with combined ST-162 and anti–PD-1 antibody when compared with vehicle control ($P < 0.0001$) or anti–PD-1 alone ($P = 0.02$; **C**), whereas no statistical significance ($P =$ NS) could be determined when compared with ST-162 alone. No statistical difference was determined between vehicle control and anti–PD-1 antibody–treated animals ($P =$ NS). **C,** Conditional survival curves of different treatment groups wherein percent change in tumor volume to 600% defined the final event. All groups were found to have significantly different times to progression ($P < 0.05$). Statistical analyses were performed in GraphPad.

(901 + ZSTK) versus cells treated with ST-162 as analyzed in more detail below.

### Comparison of gene regulation modulated by combination of kinase monotherapy versus bifunctional kinase inhibition

A heatmap of 8 genes differentially up/downregulated was generated from BrUrd data comparing A2058 melanoma cells treated with 901 + ZSTK or ST-162 (Fig. 4C). This reveals potential meaningful differences in transcriptional regulation between using a bifunctional single compound small-molecule kinase inhibitor (ST-162) targeting MEK and PI3K or a combination of two kinase inhibitors concomitantly (901 + ZSTK). Synthesis of the cysteine-rich angiogenic inducer 61 (*CYR61*) nascent RNA was upregulated (3.5 log2 fold change) in ST-162–treated cells (orange shaded) when compared with DMSO or combination drug–treated cells (Supplementary Fig. S2A). Transcription of macrophage migration inhibitory factor (*MIF*) was significantly downregulated (−5 log2 fold change) in ST-162–treated cells (green shaded) when compared wit DMSO or combinatorial treated cells (Supplementary Fig. S2B).

**Table 1.** Comparison of GI-$IC_{50}$ between A2058 and A375

| | A2058 | A375 |
|---|---|---|
| PD0325901 | 9.2 ± 1.3 nmol/L | 4.3 ± 1.2 nmol/L |
| ZSTK474 | 1,308 ± 1.2 nmol/L | 1,689 ± 1.1 nmol/L |
| ST-162 | 4,724 ± 1.1 nmol/L | 4,073 ± 1.1 nmol/L |

NOTE: Table depicts mean growth inhibitor $IC_{50}$ (GI-$IC_{50}$) values ± SEM calculated from cells treated for 72 hours with various concentrations of 901, ZSTK474, or ST-162. Presented data are compiled from three independent experiments.

### ST-162 prevents hepatic metastases

As our Bru-seq data implicated ST-162 in regulation of genes and pathways related to cell migration and metastasis, we investigated effects in a mouse model for melanoma metastases. A2058 luciferase-expressing cells were injected intracardiacally into the left ventricle of mice to produce experimental metastases. At 24 hours postinjection, we randomized mice into two groups: vehicle or 400 mg/kg ST-162 daily by oral gavage. Animals treated with ST-162 showed a significantly reduced metastatic tumor burden over time as compared with vehicle-treated animals ($P < 0.0001$; Fig. 5A and B). Histologic analysis of animals treated daily with vehicle alone at 14 days revealed large numbers of metastatic lesions in the liver (Fig. 5C). Quantification of hepatic micrometastases (number/field) from 6 different animals per group demonstrated statistical significance with a $P$ value of 0.004 (Fig. 5D). Strikingly, animals treated with the MAPK/PI3K inhibitor ST-162 showed minimal evidence of hepatic metastatic tumors with notably fewer, smaller lesions. There was no histologic evidence of lung or kidney metastatic involvement in either group. Although this experiment does not distinguish dissemination of cells to liver versus subsequent outgrowth as detectable foci of tumors, these data clearly show that ST-162 significantly reduced formation of detectable metastatic lesions in liver.

## Discussion

The conceptual development of a bifunctional MEK/PI3K inhibitor as a single chemical compound stems primarily from consideration that molecularly targeted therapy will likely be combined with existing standard-of-care chemotherapy, radiation, and/or immune therapies. Developing a single compound with activity against several different oncogenic pathways is an emerging direction for targeted agent development (29), especially in light of signaling cross-talk providing escape pathways for development of resistance. In this study, we investigated the efficacy of a novel bifunctional kinase inhibitor (ST-162),

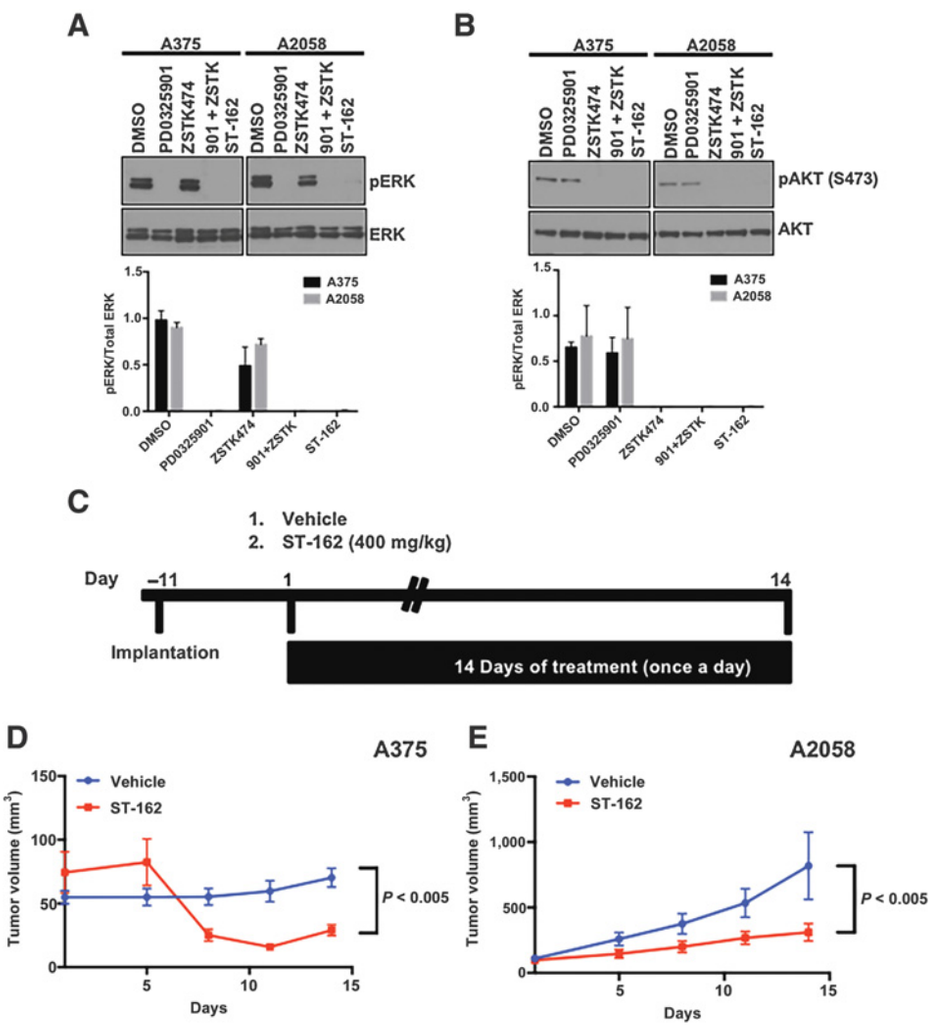


**Figure 3.**
Tumor growth inhibition by bifunctional inhibitor in PTEN wt and PTEN-null melanoma cells. **A** and **B,** Western blotting with densitometry of cell lysates obtained from melanoma cells (A375 or A2058) treated for 1 hour with 10 μmol/L 901, ZSTK, combination of both (901 + ZSTK, 10 μmol/L each), or 20 μmol/L ST-162. Presented data are compiled from two independent Western blots with mean values ± SEM. **C,** Experimental design ($n = 5$/treatment group). Treatment was initiated 11 days after A2058 (left flank) and A375 (right flank) implantation, indicated as day 1 of drug treatment. Mice were treated orally once daily for 14 days with vehicle or 400 mg/kg ST-162, respectively. **D** and **E,** Graphs show mean values ± SEM for volumes of A375 tumors (**D**) or A2058 tumors (**E**) measured by MRI in animals treated with ST-162 or vehicle. Relative to vehicle control, treatment with ST-162 significantly reduced tumor volume at the end of treatment for both cell models ($P < 0.0005$).

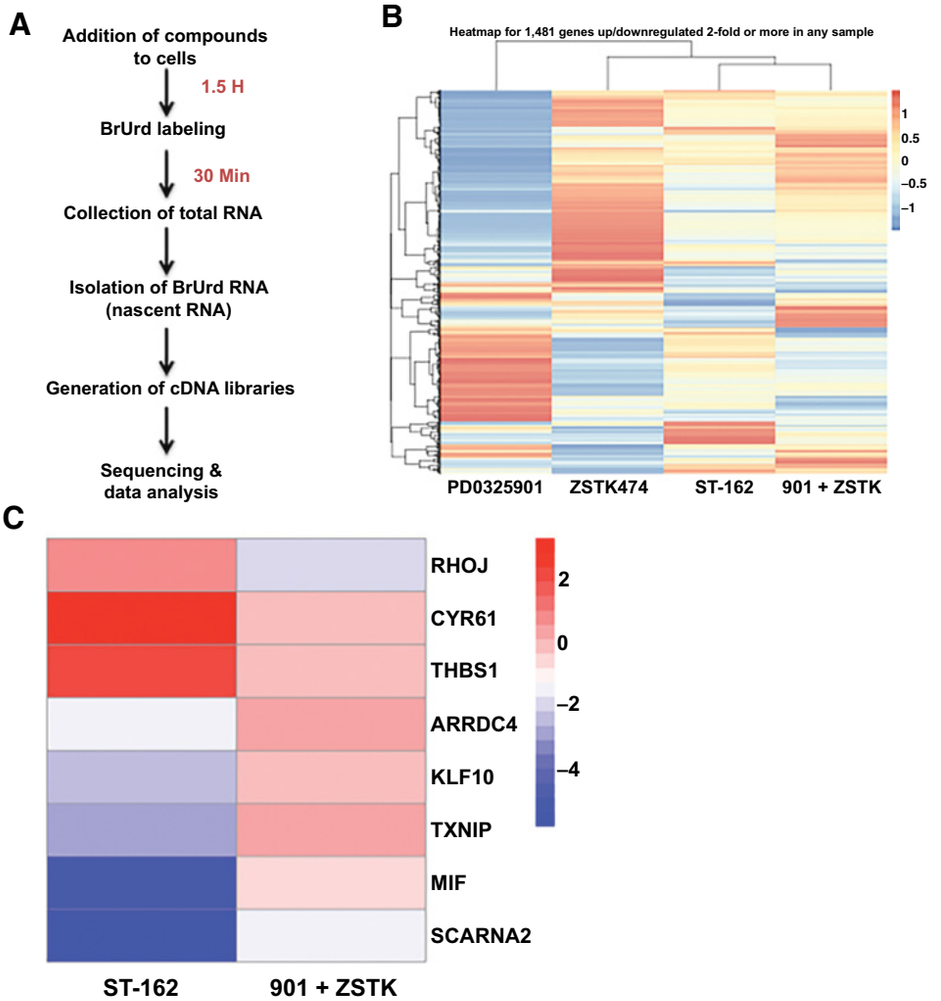


**Figure 4.**
Gene set analysis reveals common pathway regulation between combination of MEK and PI3K inhibition and bifunctional MAPK/PI3K inhibitor (ST-162). **A,** Diagram illustrating the main steps in Bru-seq. **B,** Clustered heatmap (z-scores) of 1,481 genes up/downregulated 2-fold or more in any sample. A2058 cells were treated with 10 μmol/L 901, ZSTK474, 901 + ZSTK (10 μmol/L each), or 20 μmol/L ST-162. **C,** Comparison of gene expression changes by Bru-seq modulated by combining single-kinase therapy versus bifunctional kinase inhibition. Heatmap of 8 genes differentially regulated (up/downregulated) in 901+ ZSTK treated versus ST-162–treated melanoma A2058 cells.

showing antitumor activity in colorectal cancer and melanoma mouse models. Combining ST-162 with immune checkpoint inhibition demonstrated therapeutic efficacy over anti–PD-1 treatment alone. Moreover, nascent RNA transcriptomics revealed a subset of genes regulated by ST-162, providing potential mechanisms underlying efficacy of this compound against a melanoma hepatic metastases model.

Current clinical trials targeting both MEK and PI3K involve an attempt to optimize dose and schedule to yield suitable safety and tolerability. Limitations of "combination therapy" include dissimilar toxicity profiles, pharmacokinetics as well as issues with patient compliance (27, 30–33). A recent phase Ib trial evaluating the MEK inhibitor trametinib in combination with the PI3K/mTOR inhibitor GSK2126458 in patients with advanced solid tumors reported minimal responses and significant overlapping toxicities (34). Additional clinical trials using combinations of PI3K/AKT and MEK inhibitors show poor tolerability, significant and overlapping side effects, and limited antitumor efficacy (34–41). Our effort toward development of an anticancer therapeutic for dual inhibition of these two key signaling pathways has focused on a bifunctional single-agent therapeutic (ST-162), which potentially may improve efficacy in the treatment of melanomas by simplifying treatment regimens and reducing toxicity.

Results from colorectal and melanoma mouse xenograft models show tolerance of ST-162 at doses of 400 mg/kg administered orally with no observed toxicities as assessed by changes in animal weight. ADME (absorption, distribution, metabolism, and excretion) studies of ST-162 will be undertaken in future studies to optimize dose and schedule. However, in a preliminary necropsy study accomplished in our laboratory following dosing of mice with ST-162 at 400 mg/kg/day for 30 days continuously found no adverse histologic or hematologic effects noted by a pathologist. Although further work will be required to improve the formulation and dosing schedule, our ST-162 results to date are highly encouraging.

Although GI-$IC_{50}$s for ST-162 were in the micromolar range and notably higher when compared with single agents 901 and ZSTK, we demonstrated similar efficacy profiles to combination therapy in various mouse cancer models. These data support design of a single therapeutic agent targeting multiple kinases. Efforts are ongoing to improve solubility and formulation of ST-162 in an effort to further optimize GI-$IC_{50}$ for cell-based and animal studies.

ST-162 caused tumor regression in A374 melanoma xenografts, but only tumor growth inhibition or tumor stasis could be achieved in cells harboring BRAF and PTEN mutations. This

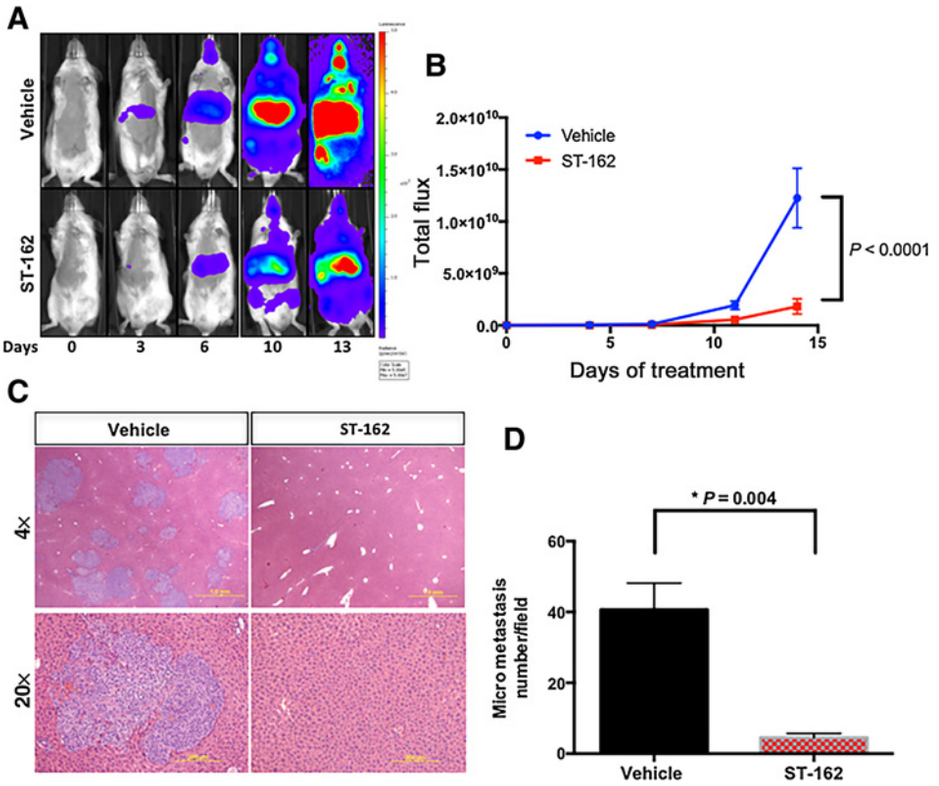


**Figure 5.**
Effects of MAPK/PI3K inhibition on migratory properties of melanoma cells. We injected A2058-luciferase cells via the left cardiac ventricle and imaged tumor burden by bioluminescence imaging immediately after injection and then on days 3, 6, 10, and 13. A total of 20 NSG mice were injected and randomized into two groups ($n = 10$/group). **A,** Representative bioluminescence images are shown for each group at different time points. **B,** Total flux was plotted for vehicle-treated animals (blue) or animals treated daily with 400 mg/kg of ST-162 over the course of 14 days. Statistical significance ($P < 0.0001$) was determined between vehicle control and ST-162–treated animals at the end of treatment. **C,** Microscopic images (×4 and ×20) of H&E staining from hepatic tissue of animals treated with vehicle or ST-162 on day 14. **D**, Quantification of micrometastases (number/field) from 6 different mice per group. Group comparisons were performed using an unpaired Student *t* test. Statistical significance was assessed at $P < 0.05$ using GraphPad software.

difference in efficacy likely reflects activation of AKT/mTOR signaling downstream of PI3K. This underscores the importance of patient stratification based on existing mutations in tumor tissue for selecting the optimal therapy. Agents targeting cell proliferative pathways may not induce tumor cell death or induce significant tumor regression. However, these agents may induce cell-cycle arrest or senescence, thereby prolonging survival by delaying disease progression (42). Nevertheless, inhibition of MAPK/PI3K pathway by ST-162 in a melanoma metastases model prevented hepatic metastases despite PTEN mutation status in those cells. PI3K/AKT signaling has previously been demonstrated to play a substantial role in the formation of metastases by mediating a switch to an aggressive/metastatic melanoma phenotype (25, 43), but the data presented here indicate possible additional mechanisms of metastases via PI3K regulation may be involved.

Combining targeted agents with immune checkpoint blockade has emerged as a promising new anticancer approach. For example, treatment with a MEK/BRAF inhibitor plus an immune checkpoint modulator improved control of colorectal tumors (21). Our data indicate that immune checkpoint inhibition improves efficacy of ST-162 therapy. However, further work is required to optimize combination therapy with ST-162 and immunotherapy, particularly in the context of tumors with drug resistance.

Comprehensive nascent transcriptome studies comparing MEK inhibition to PI3K inhibition in a melanoma cell line demonstrated both expected and novel changes in gene transcription. Interestingly, ST-162 profiles were more similar to profiles from ZSTK-treated cells or cells treated with combinations of the two single agents (901 + ZSTK). The apparent difference of the MEK inhibitor (901)–treated cell profile identified by clustering from all other treatments may indicate potential off-target effects due to the relatively high doses used in this experiment (10 μmol/L) for 901. However, we observed expected changes in gene transcription, for example, mTOR and PI3K pathway signaling was upregulated in MEK-inhibited cells using 901, which was not observed in cells treated with a combination of 901 + ZSTK or ST-162. These data support previously described pathway cross-talk and emerging resistance through upregulation of the PI3K/AKT/mTOR signaling axis. All samples treated with the PI3K inhibitor ZSTK showed upregulation of p53 signaling, likely due to inhibition of AKT blocking MDM2-mediated degradation of p53 (44). p53 signaling and cell division also activate DNA repair mechanisms. Intriguing findings from transcriptome analysis reveal pathway downregulations of TGFβ signaling in MEK-inhibited cells, which may have potential implications for cross-talk between cancer cells and the immune system. In addition, although apoptosis appeared unenriched by our studies in 3 of 4 conditions, further functional studies would be required to support the case for combining targeted agents with cytotoxic therapies to achieve maximal therapeutic benefit.

Our comparative genetic findings show unique modulatory effects on signaling pathways versus single-agent combinations. However, as a direct comparison between GI-$IC_{50}$ of ST-162 and combination-treated cells (901 + ZSTK) was not performed, the possibility cannot be ruled out that observed effects on gene transcription could be due to differences in pathway inhibition by off-target effects as the doses used to perform Bru-seq transcriptome studies were higher than those determined for GI-$IC_{50}$ for single agents and ST-162. Nevertheless, we identified differential regulation of genes, including *CYR61* and *MIF*. *CYR61* has

been described as a tumor suppressor of melanoma cell mobility, invasion, and angiogenesis (45), whereas *MIF* depletion decreased proliferation, anchorage-independent growth and increased apoptosis (46). These differentially expressed genes suggest potential mechanisms for almost complete absence of detectable metastatic lesions in livers of mice treated with ST-162. Although our preliminary results require further functional valuation, the potentially unique genetic and pathway regulation by ST-162 may offer therapeutic advantages over single agent or combined MEK and PI3K inhibitors, including antimetastatic activity.

In summary, we have developed ST-162 as an efficacious bifunctional kinase inhibitor that prevents tumor growth in KRAS- and BRAF-mutated cells, induces tumor stasis in BRAF PTEN-mutated cells, and inhibits metastases possibly through regulating a unique set of genes.

## Disclosure of Potential Conflicts of Interest

M. Van Dort has ownership interest (including patents) in the University of Michigan. B.D. Ross is the founder and chief scientific officer at and has ownership interest (including patents) in Sarisa, LLC. No potential conflicts of interest were disclosed by the other authors.

## Authors' Contributions

**Conception and design:** S. Galbán, G.D. Luker, M. Van Dort, B.D. Ross
**Development of methodology:** S. Galbán
**Acquisition of data (provided animals, acquired and managed patients, provided facilities, etc.):** S. Galbán, A.A. Apfelbaum, C. Espinoza, K. Heist, H. Haley, M. Ljungman
**Analysis and interpretation of data (e.g., statistical analysis, biostatistics, computational analysis):** S. Galbán, A.A. Apfelbaum, C. Espinoza, K. Bedi, M. Ljungman, C.J. Galbán, B.D. Ross
**Writing, review, and/or revision of the manuscript:** S. Galbán, A.A. Apfelbaum, K. Bedi, M. Ljungman, C.J. Galbán, G.D. Luker, M. Van Dort, B.D. Ross
**Administrative, technical, or material support (i.e., reporting or organizing data, constructing databases):** S. Galbán, K. Heist
**Study supervision:** S. Galbán, G.D. Luker, M. Van Dort, B.D. Ross
**Other (designed and developed key drug used in study):** M. Van Dort

## Acknowledgments

The authors wish to thank Michelle Paulsen for technical expertise with Bru-seq and Rachel Lombardi, Karamoja Monchamp, Elliot Marshallsay, Charlie Nino, John Vorwald, and Philip Reed for assisting with experiments and critical reading of the manuscript.

## Grant Support

This work was supported in part by NIH/NCI grants P01CA085878, R35CA197701, R01CA170198, R01CA196018, and R01CA195655.

The costs of publication of this article were defrayed in part by the payment of page charges. This article must therefore be hereby marked *advertisement* in accordance with 18 U.S.C. Section 1734 solely to indicate this fact.

Received March 6, 2017; revised May 8, 2017; accepted July 20, 2017; published OnlineFirst August 3, 2017.

## References

1. Singer DS, Jacks T, Jaffee E. A U.S. "Cancer Moonshot" to accelerate cancer research. Science 2016;353:1105–6.
2. Baines AT, Xu D, Der CJ. Inhibition of Ras for cancer treatment: the search continues. Future Med Chem 2011;3:1787–808.
3. Mirzoeva OK, Das D, Heiser LM, Bhattacharya S, Siwak D, Gendelman R, et al. Basal subtype and MAPK/ERK kinase (MEK)-phosphoinositide 3-kinase feedback signaling determine susceptibility of breast cancer cells to MEK inhibition. Cancer Res 2009;69:565–72.
4. Castellano E, Downward J. RAS interaction with PI3K: more than just another effector pathway. Genes Cancer 2011;2:261–74.
5. Serra V, Scaltriti M, Prudkin L, Eichhorn PJ, Ibrahim YH, Chandarlapaty S, et al. PI3K inhibition results in enhanced HER signaling and acquired ERK dependency in HER2-overexpressing breast cancer. Oncogene 2011;30: 2547–57.
6. Aksamitiene E, Kiyatkin A, Kholodenko BN. Cross-talk between mitogenic Ras/MAPK and survival PI3K/Akt pathways: a fine balance. Biochem Soc Trans 2012;40:139–46.
7. Chandarlapaty S. Negative feedback and adaptive resistance to the targeted therapy of cancer. Cancer Discov 2012;2:311–9.
8. Turke AB, Song Y, Costa C, Cook R, Arteaga CL, Asara JM, et al. MEK inhibition leads to PI3K/AKT activation by relieving a negative feedback on ERBB receptors. Cancer Res 2012;72:3228–37.
9. Guenther MK, Graab U, Fulda S. Synthetic lethal interaction between PI3K/Akt/mTOR and Ras/MEK/ERK pathway inhibition in rhabdomyosarcoma. Cancer Lett 2013;337:200–9.
10. Populo H, Soares P, Rocha AS, Silva P, Lopes JM. Evaluation of the mTOR pathway in ocular (uvea and conjunctiva) melanoma. Melanoma Res 2010;20:107–17.
11. Saraiva VS, Caissie AL, Segal L, Edelstein C, Burnier MN Jr. Immunohistochemical expression of phospho-Akt in uveal melanoma. Melanoma Res 2005;15:245–50.
12. Gross S, Rahal R, Stransky N, Lengauer C, Hoeflich KP. Targeting cancer with kinase inhibitors. J Clin Invest 2015;125:1780–9.
13. Van Dort ME, Hong H, Wang H, Nino CA, Lombardi RL, Blanks AE, et al. Discovery of bifunctional oncogenic target inhibitors against allosteric mitogen-activated protein kinase (MEK1) and phosphatidylinositol 3-kinase (PI3K). J Med Chem 2016;59:2512–22.
14. Xiao A, Gibbons AE, Luker KE, Luker GD. Fluorescence lifetime imaging of apoptosis. Tomography 2015;1:115–24.
15. Paulsen MT, Veloso A, Prasad J, Bedi K, Ljungman EA, Magnuson B, et al. Use of Bru-Seq and BruChase-Seq for genome-wide assessment of the synthesis and stability of RNA. Methods 2014;67:45–54.
16. Paulsen MT, Veloso A, Prasad J, Bedi K, Ljungman EA, Tsan YC, et al. Coordinated regulation of synthesis and stability of RNA during the acute TNF-induced proinflammatory response. Proc Natl Acad Sci U S A 2013;110:2240–5.
17. Fenner J, Stacer AC, Winterroth F, Johnson TD, Luker KE, Luker GD. Macroscopic stiffness of breast tumors predicts metastasis. Sci Rep 2014;4:5512.
18. Yoon YK, Kim HP, Han SW, Oh DY, Im SA, Bang YJ, et al. KRAS mutant lung cancer cells are differentially responsive to MEK inhibitor due to AKT or STAT3 activation: implication for combinatorial approach. Mol Carcinog 2010;49:353–62.
19. Frederick DT, Piris A, Cogdill AP, Cooper ZA, Lezcano C, Ferrone CR, et al. BRAF inhibition is associated with enhanced melanoma antigen expression and a more favorable tumor microenvironment in patients with metastatic melanoma. Clin Cancer Res 2013;19:1225–31.
20. Kim T, Amaria RN, Spencer C, Reuben A, Cooper ZA, Wargo JA. Combining targeted therapy and immune checkpoint inhibitors in the treatment of metastatic melanoma. Cancer Biol Med 2014;11:237–46.
21. Liu L, Mayes PA, Eastman S, Shi H, Yadavilli S, Zhang T, et al. The BRAF and MEK inhibitors dabrafenib and trametinib: effects on immune function and in combination with immunomodulatory antibodies targeting PD-1, PD-L1, and CTLA-4. Clin Cancer Res 2015; 21:1639–51.
22. Barrett SD, Bridges AJ, Dudley DT, Saltiel AR, Fergus JH, Flamme CM, et al. The discovery of the benzhydroxamate MEK inhibitors CI-1040 and PD 0325901. Bioorg Med Chem Lett 2008;18:6501–4.
23. Yaguchi S, Fukui Y, Koshimizu I, Yoshimi H, Matsuno T, Gouda H, et al. Antitumor activity of ZSTK474, a new phosphatidylinositol 3-kinase inhibitor. J Natl Cancer Inst 2006;98:545–56.
24. Deuker MM, Marsh Durban V, Phillips WA, McMahon M. PI3′-kinase inhibition forestalls the onset of MEK1/2 inhibitor resistance in BRAF-mutated melanoma. Cancer Discov 2015;5:143–53.

25. Cho JH, Robinson JP, Arave RA, Burnett WJ, Kircher DA, Chen G, et al. AKT1 activation promotes development of melanoma metastases. Cell Rep 2015;13:898–905.
26. Welsh SJ, Rizos H, Scolyer RA, Long GV. Resistance to combination BRAF and MEK inhibition in metastatic melanoma: where to next? Eur J Cancer 2016;62:76–85.
27. Hoeflich KP, Merchant M, Orr C, Chan J, Den Otter D, Berry L, et al. Intermittent administration of MEK inhibitor GDC-0973 plus PI3K inhibitor GDC-0941 triggers robust apoptosis and tumor growth inhibition. Cancer Res 2012;72:210–9.
28. Catalanotti F, Solit DB, Pulitzer MP, Berger MF, Scott SN, Iyriboz T, et al. Phase II trial of MEK inhibitor selumetinib (AZD6244, ARRY-142886) in patients with BRAFV600E/K-mutated melanoma. Clin Cancer Res 2013; 19:2257–64.
29. Rodrik-Outmezguine VS, Okaniwa M, Yao Z, Novotny CJ, McWhirter C, Banaji A, et al. Overcoming mTOR resistance mutations with a new-generation mTOR inhibitor. Nature 2016;534:272–6.
30. Van Dort ME, Galban S, Wang H, Sebolt-Leopold J, Whitehead C, Hong H, et al. Dual inhibition of allosteric mitogen-activated protein kinase (MEK) and phosphatidylinositol 3-kinase (PI3K) oncogenic targets with a bifunctional inhibitor. Bioorg Med Chem 2015;23:1386–94.
31. Renshaw J, Taylor KR, Bishop R, Valenti M, De Haven Brandon A, Gowan S, et al. Dual blockade of the PI3K/AKT/mTOR (AZD8055) and RAS/MEK/ERK (AZD6244) pathways synergistically inhibits rhabdomyosarcoma cell growth *in vitro* and *in vivo*. Clin Cancer Res 2013;19:5940–51.
32. Knight ZA, Lin H, Shokat KM. Targeting the cancer kinome through polypharmacology. Nat Rev Cancer 2010;10:130–7.
33. Zhang X, Zhang J, Tong L, Luo Y, Su M, Zang Y, et al. The discovery of colchicine-SAHA hybrids as a new class of antitumor agents. Bioorg Med Chem 2013;21:3240–4.
34. Grilley-Olson JE, Bedard PL, Fasolo A, Cornfeld M, Cartee L, Razak AR, et al. A phase Ib dose-escalation study of the MEK inhibitor trametinib in combination with the PI3K/mTOR inhibitor GSK2126458 in patients with advanced solid tumors. Invest New Drugs 2016;34:740–9.
35. Bedard P, Tabernero J, Kurzrock R, Britten CD, Stathis A, Perez-Garcia JM, et al. A phase Ib, open-label, multicenter, dose-escalation study of the oral pan-PI3K inhibitor BKM120 in combination with the oral MEK1/2 inhibitor GSK1120212 in patients (pts) with selected advanced solid tumors. J Clin Oncol 30:15s, 2012(suppl; abstr 3003).
36. Bendell JC, LoRusso P, Cho DC, Musib L, Yan Y, Chang I, et al. Clinical results of a phase Ib dose-escalation study of the Mek inhibitor cobimetinib (GDC-0973) and the Akt inhibitor ipatasertib (GDC-0068) in patients (pts) with solid tumors. In: Proceedings of the 105th Annual Meeting of the American Association for Cancer Research; 2014 Apr 5–9; San Diego, CA. Philadelphia (PA): AACR; 2014. Abstract nr CT328.
37. Infante JR, Gandhi L, Shapiro G, Burris HA, Bendell JC, Baselga J, et al. Phase Ib combination trial of a MEK inhibitor, pimasertib (MSC1936369B), and a PI3K/mTOR inhibitor, SAR245409, in patients with locally advanced or metastatic solid tumors. J Clin Oncol 30:15s, 2012(suppl; abstr TPS3118).
38. Kurzrock R, Patnaik A, Rosenstein L, Fu S, Papadopoulos K, Smith D, et al. Phase I dose-escalation of the oral MEK1/2 inhibitor GSK1120212 (GSK212) dosed in combination with the oral AKT inhibitor GSK2141795 (GSK795). J Clin Oncol 29:15s, 2011(suppl; abstr 3085).
39. Shapiro G, LoRusso P, Kwak E, Cleary J, Musib L, Jones C, et al. Clinical combination of the MEK inhibitor GDC-0973 and the PI3K inhibitor GDC-0941: A first-in-human phase Ib study testing daily and intermittent dosing schedules in patients with advanced solid tumors. J Clin Oncol 29:15s, 2011(suppl; abstr 3005).
40. Tolcher A, Baird R, Patnaik A, Moreno Garcia V, Papadopoulos K, Garrett C, et al. A phase I dose-escalation study of oral MK-2206 (allosteric AKT inhibitor) with oral selumetinib (AZD6244; MEK inhibitor) in patients with advanced or metastatic solid tumors. J Clin Oncol 29:15s, 2011 (suppl; abstr 3004).
41. Tolcher AW, Patnaik A, Papadopoulos KP, Rasco DW, Becerra CR, Allred AJ, et al. Phase I study of the MEK inhibitor trametinib in combination with the AKT inhibitor afuresertib in patients with solid tumors and multiple myeloma. Cancer Chemother Pharmacol 2015;75:183–9.
42. Solit DB, Santos E, Pratilas CA, Lobo J, Moroz M, Cai S, et al. 3′-deoxy-3′-[18F]fluorothymidine positron emission tomography is a sensitive method for imaging the response of BRAF-dependent tumors to MEK inhibition. Cancer Res 2007;67:11463–9.
43. Smalley KS, Fedorenko IV. Inhibition of BRAF and BRAF+MEK drives a metastatic switch in melanoma. Mol Cell Oncol 2015;2:e1008291.
44. Feng J, Tamaskovic R, Yang Z, Brazil DP, Merlo A, Hess D, et al. Stabilization of Mdm2 via decreased ubiquitination is mediated by protein kinase B/Akt-dependent phosphorylation. J Biol Chem 2004;279:35510–7.
45. Dobroff AS, Wang H, Melnikova VO, Villares GJ, Zigler M, Huang L, et al. Silencing cAMP-response element-binding protein (CREB) identifies CYR61 as a tumor suppressor gene in melanoma. J Biol Chem 2009; 284:26194–206.
46. Oliveira CS, de Bock CE, Molloy TJ, Sadeqzadeh E, Geng XY, Hersey P, et al. Macrophage migration inhibitory factor engages PI3K/Akt signalling and is a prognostic factor in metastatic melanoma. BMC Cancer 2014;14:630.